

Electronic Supplementary Information

The first Re^I organometallic complex with an organoimido-polyoxometalate ligand.

Patricio Hermosilla-Ibáñez,^{a,b} Kerry Wrighton-Araneda,^{a,b} Gaspar Prado,^c Verónica Paredes-García,^{b,c} Nancy Pizarro,^c Andrés Vega^{*b,c} and Diego Venegas-Yazigi^{*a,b}.

^{a)} Universidad de Santiago de Chile, Facultad de Química y Biología, Departamento de Química de los Materiales, (IPMag), Chile.

^{b)} Centro para el Desarrollo de la Nanociencia y la Nanotecnología, CEDENNA, Chile..

^{c)} Universidad Andres Bello, Facultad de Ciencias Exactas, Departamento de Ciencias Químicas, (IPMag), Chile.

E-mail: diego.venegas@usach.cl; Tel:(+56-2-27181079

Table S1. Crystal parameters and refinement details for **1**

Empirical Formula	C ₄₁ H ₈₀ Mo ₆ N ₆ O ₁₈
Formula weight	1520.75
Temperature/K	296(2)
Crystal system	Triclinic
Space group	<i>P</i> 1
a/Å	11.835(3)
b/Å	14.997(4)
c/Å	16.445(4)
α/°	85.180(3)
β/°	84.602(3)
γ/°	82.019(3)
Volume/Å ³	2870.4(12)
Z	2
ρ _{calc} g/cm ³	1.760
μ/mm ⁻¹	1.340
F(000)	1528.0
Crystal size/mm ³	0.10 × 0.05 × 0.05
Radiation	MoKα ($\lambda = 0.71073$)
2Θ range for data collection/°	4.454 to 54
Index ranges	-15 ≤ h ≤ 15, -19 ≤ k ≤ 19, -20 ≤ l ≤ 20
Reflections collected	92492
Independent reflections	24951 [R _{int} = 0.1095, R _{sigma} = 0.1181]
Data/restraints/parameters	24951/263/1367
Goodness-of-fit on F ²	1.004
Final R indexes [I>=2σ (I)]	R ₁ = 0.0604, wR ₂ = 0.1093
Final R indexes [all data]	R ₁ = 0.1506, wR ₂ = 0.1445
Largest diff. peak/hole / e Å ⁻³	0.57/-0.56

Table S2. Shape calculation of the continuous shape measurements of all molybdenum atoms of the two POMs. HP-6 (Hexagon); PPY-6 (Pentagonal pyramid); OC-6 (Octahedron); TPR-6 (Trigonal prism); JPPY-6 (Johnson pentagonal pyramid J2).

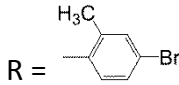
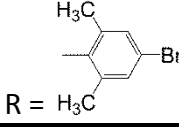
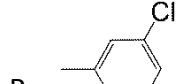
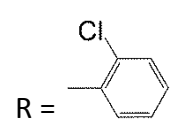
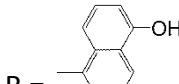
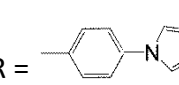
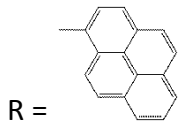
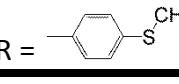
ML₆-unit I	HP-6	PPY-6	OC-6	TPR-6	JPPY-6
Mo1	33.822	29.71	0.939	17.016	33.205
Mo2	33.614	29.465	0.888	16.599	32.984
Mo3	33.703	29.71	0.893	16.823	33.133
Mo4N	33.134	29.447	0.649	16.741	33.008
Mo5	33.287	29.6	0.898	16.875	32.982
Mo6	33.669	29.548	0.867	17.059	33.035

ML₆-unit II	HP-6	PPY-6	OC-6	TPR-6	JPPY-6
Mo7	33.227	29.666	0.833	16.842	33.132
Mo8	33.456	29.608	0.874	17.025	32.914
Mo9	33.617	29.529	0.912	16.786	33.044
Mo10	33.198	29.013	0.886	16.672	32.425
Mo11N	32.648	29.75	0.672	16.902	33.046
Mo12	33.136	29.301	1.018	16.731	32.521

Table S3. ^1H -NMR signals of compounds **1** and **2**. The letters indicates to what protons are related the signals.

Signals	1	2	
	δ / ppm	δ / ppm	
a	0.91	0.90	t, -CH ₃ , [n-Bu ₄ N] ⁺
b	1.28	1.25	m, -CH ₂ -, [n-Bu ₄ N] ⁺
c	1.52	1.51	m, -CH ₂ -, [n-Bu ₄ N] ⁺
d	3.14	3.13	t, N-CH ₂ -, [n-Bu ₄ N] ⁺
e	5.16	4.88, 5.74	s, N-CH ₂ -C
f	6.51	6.33	d, aromatic
g	6.98	6.57	d, aromatic
h	7.92	8.02	s, N-CH-N
i	8.53	8.80	s, N-CH-N
j	-	8.17	dd, phen
k	-	8.31	s, phen
l	-	9.01	dd, phen
m	-	9.61	dd, phen

Table S4. Summary of cathodic shifts ($\Delta E_{1/2}$) for the first reduction potential of hexamolybdates functionalized with different organoimido groups. All values were compared with the reduction potential of hexamolybdate $[\text{Mo}_6\text{O}_{19}]^{2-}$.

$\Delta E_{1/2} / \text{mV}$	$\text{Mo}_6\text{O}_{18}\text{N}-\text{R}$	References
271	$\text{R} = -\text{CH}_3$	
307	$\text{R} = -\text{C}(\text{CH}_3)_3$	1
270	$\text{R} = -\text{CH}_2-(\text{CH}_2)_4-\text{CH}_3$	
189	$\text{R} =$ 	2
212	$\text{R} =$ 	
191	$\text{R} =$ 	3
197	$\text{R} =$ 	
258	$\text{R} =$ 	4
185	$\text{R} =$ 	5
452	$\text{R} =$ 	6
174	$\text{R} =$ 	7

References

- 1 Q. Li, L. Wang, P. Yin, Y. Wei, J. Hao, Y. Zhu, L. Zhu and G. Yuan, *Dalton Trans.*, 2009, **18**, 1172–1179.
- 2 Q. Li, L. Zhu, X. Meng, Y. Zhu, J. Hao and Y. Wei, *Inorg. Chim. Acta*, 2007, **360**, 2558–2564.
- 3 Q. Li, Y. Wei, H. Guo and C.-G. Zhan, *Inorg. Chim. Acta*, 2008, **361**, 2305–2313.
- 4 L. Wang, L. Zhu, P. Yin, W. Fu, J. Chen, J. Hao, F. Xiao, C. Lv, J. Zhang, L. Shi, Q. Li and Y. Wei, *Inorg. Chem.*, 2009, **48**, 9222–9235.

- 5 A. Al-Yasari, N. Van Steerteghem, H. El Moll, K. Clays and J. Fielden, *Dalton Trans.*, 2016, **45**, 2818–2822.
- 6 J. Gao, X. Liu, Y. Liu, L. Yu, Y. Feng, H. Chen, Y. Li, G. Rakesh, C. H. A. Huan, T. C. Sum, Y. Zhao and Q. Zhang, *Dalton Trans.*, 2012, **41**, 12185–12191.
- 7 H. Guo, S.-Z. Li, X.-X. Xiong, D. Li, Z.-Y. Liu, L.-S. Wang and P.-F. Wu, *Polyhedron*, 2015, **92**, 1–6.

Table S5. Summary of calculated and experimental redox potentials for the first reduction process.

Reaction	$E_{\text{redox}} / \text{V}$	Shift $E_{\text{redox}} / \text{mV}$	$E_{1/2} / \text{V}$	Shift
			Exp.	$E_{1/2} / \text{mV}$
$[\text{Mo}_5^{\text{VI}}\text{O}_{19}]^{2-} + \text{e} \rightarrow [\text{Mo}_5^{\text{VI}}\text{Mo}_1^{\text{V}}\text{O}_{19}]^{3-}$	-0.6867	-	-0.801	-
$[\text{Mo}_6^{\text{VI}}\text{O}_{18}-\text{NC}_6\text{H}_4-\text{CH}_2-\text{N}_3\text{C}_2\text{H}_2]^{2-} + \text{e} \rightarrow$ $[\text{Mo}_5^{\text{VI}}\text{Mo}_1^{\text{V}}\text{O}_{18}-\text{NC}_6\text{H}_4-\text{CH}_2-\text{N}_3\text{C}_2\text{H}_2]^{3-}$	-0.9389	252	-1.011	175
$[\text{Mo}_6^{\text{VI}}\text{O}_{18}\text{NC}_6\text{H}_4-\text{CH}_2-\text{N}_3\text{C}_2\text{H}_2-\text{RePhen}(\text{CO})_3] + \text{e} \rightarrow$ $[\text{Mo}_5^{\text{VI}}\text{Mo}_1^{\text{V}}\text{O}_{18}\text{NC}_6\text{H}_4-\text{CH}_2-\text{N}_3\text{C}_2\text{H}_2-\text{RePhen}(\text{CO})_3]^{2-}$	-0.9108	224	-0.911	130
.				

Table S6. Summary of charges condensed to atoms employing MPA, NPA, APTPA and HPA for the constituent fragment of **Mo₆**, **1** and **2**.

Compound	Fragment	MPA	NPA	APTPA	HPA
Mo₆	Mo ₆ O ₁₈	-1.490	-1.589	-0.729	-1.753
	O	-0.510	-0.411	-1.271	-0.247
1	Mo ₆ O ₁₈	-1.648	-1.982	-1.325	-2.056
	NC ₆ H ₄ -CH ₂ -N ₃ C ₂ H ₂	-0.352	-0.018	-0.675	+0.056
2	Mo ₆ O ₁₈	-1.638	-1.973	-1.289	-2.047
	NC ₆ H ₄ -CH ₂ -N ₃ C ₂ H ₂	-0.008	+0.310	-0.451	+0.441
	Rephen(CO) ₃	+0.647	+0.663	+0.740	+0.606
1-Mo₆	Mo ₆ O ₁₈	-0.158	-0.393	-0.596	-0.303
2-Mo₆	Mo ₆ O ₁₈	-0.148	-0.384	-0.560	-0.294
2-1	Mo ₆ O ₁₈	+0.010	+0.009	+0.036	+0.009
2-1	NC ₆ H ₄ -CH ₂ -N ₃ C ₂ H ₂	+0.344	+0.328	+0.224	+0.385

MPA: Mulliken Population Analysis

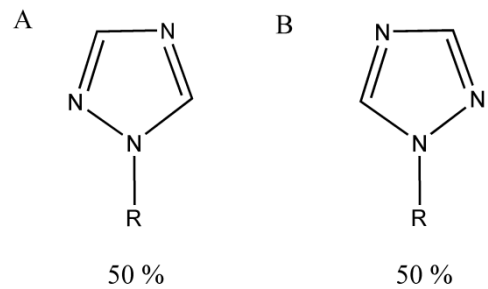
NPA: Natural Population Analysis

APTPA: Atomic Polar Tensor Population Analysis

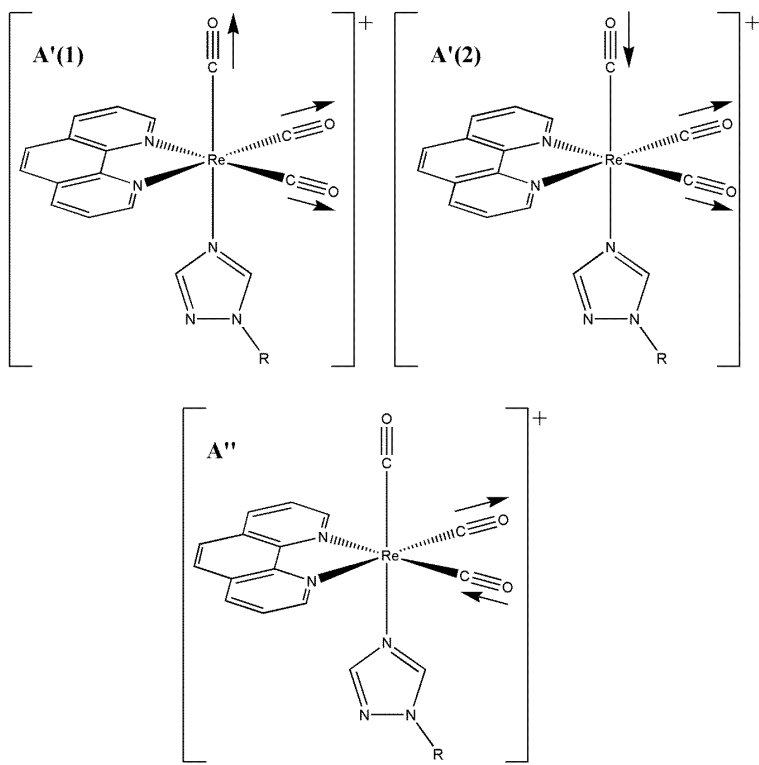
HPA: Hirshfeld Population Analysis

Table S7. Electronic parameters of the most intensive excitation corresponding to **Mo₆**, **1** and **2**.

Compound	Wavelength	Oscillator nm	Assignment		% Contribution
			Strength		
Mo₆	313.3	0.050	HOMO - 1	→ LUMO	44
			HOMO	→ LUMO + 1	42
			HOMO - 4	→ LUMO + 2	8
1	346.5	0.377	HOMO	→ LUMO + 6	84
2	345.4	0.398	HOMO	→ LUMO + 7	76
			HOMO - 1	→ LUMO + 7	8



Scheme S1. Nitrogen location possibilities for the 1,2,4-triazole ring in **1**.



Scheme S2. A'(1), A'(2), and A'' normal modes in C_s symmetry.

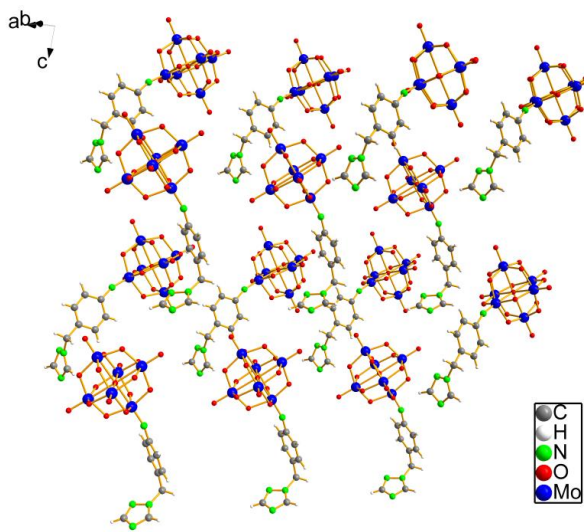


Figure S1. Crystal packing of compound **1**, showing the spatial disposition of the two different organoimido polyoxomolybdates units. $[n\text{-Bu}_4\text{N}]^+$ were omitted for clarity.

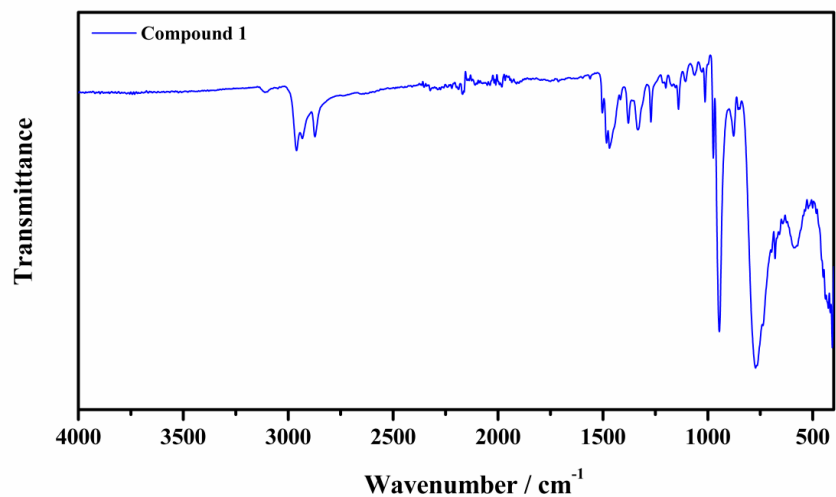


Figure S2. FTIR-ATR spectrum in the 400 to 4000 cm^{-1} region of compound 1 (blue).

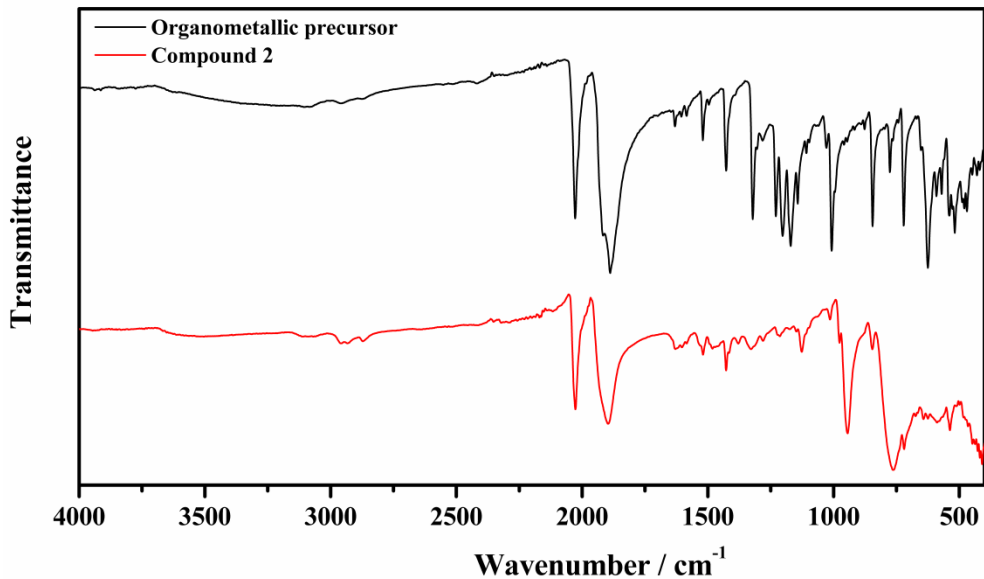


Figure S3. FTIR-ATR spectra of **2** (red) and organometallic precursor *fac*-[(phen)(H₂O)Re(CO)₃]⁺(CF₃SO₃)⁻ (black), in the 400 to 4000 cm⁻¹ region.

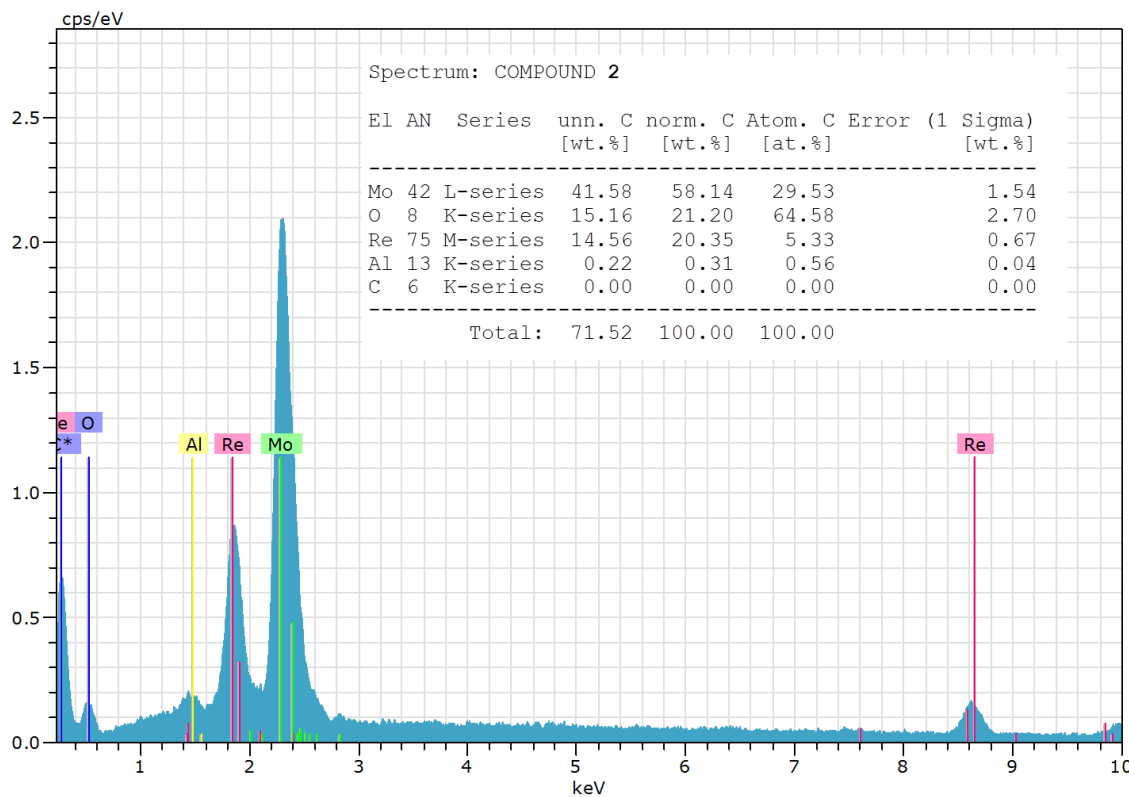


Figure S4. EDX spectrum of [n-Bu₄N][Mo₆O₁₈NC₆H₄-CH₂-N₃C₂H₂-Re(phen)(CO)₃] (**2**).

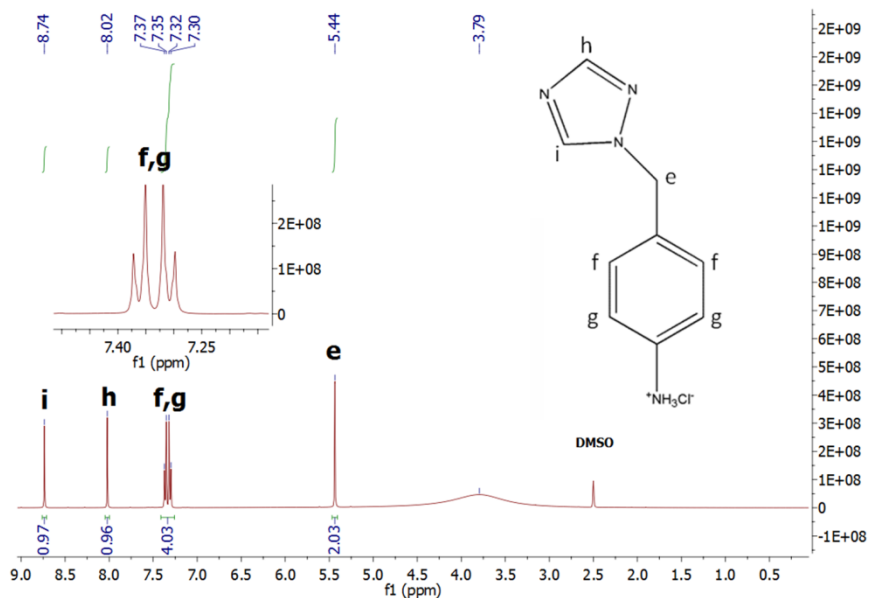


Figure S5. The ^1H -NMR spectrum of hydrochloride salt of 4-(1,2,4-triazolylmethyl)phenylamine (d_6 -DMSO). Inset scheme showing the protons assignments to amine ligand.

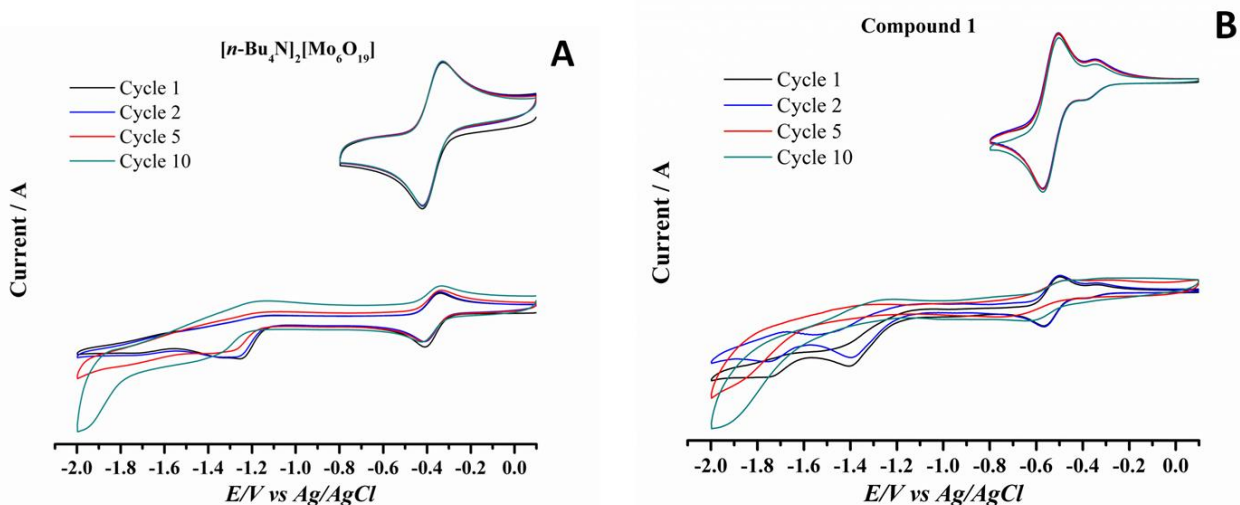


Figure S6. Cyclic voltammograms of the hexamolybdate (black) compared to compounds **1** (red) and **2** (blue) measured in CH_3CN and ($n\text{-Bu}_4\text{NClO}_4$) as the supporting electrolyte at scan rate of 100 mV/s.

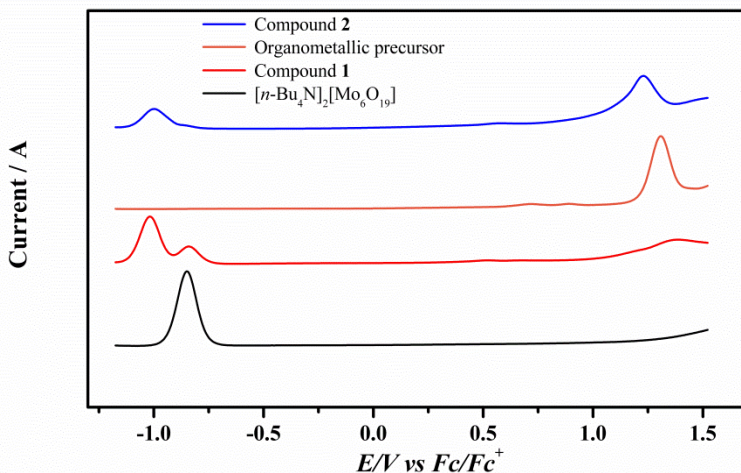


Figure S7. Square-Wave voltamograms of compound **1** (red), compound **2** (blue), hexamolybdate (black) and organometallic precursor *fac*-[(phen)(H₂O)Re(CO)₃]⁺ (orange) measured in CH₃CN and (n-Bu₄N)ClO₄ as the supporting electrolyte. All measurement were referred to Fc/Fc⁺ potential.

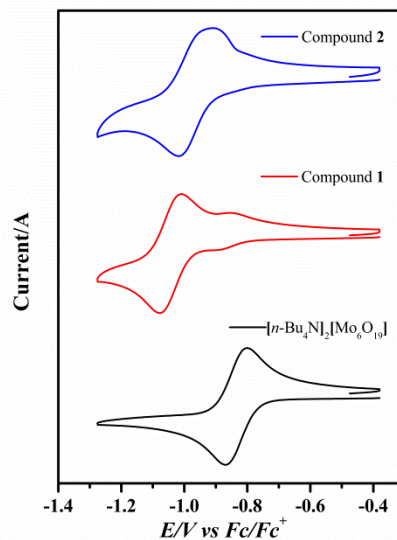


Figure S8. Cyclic voltamograms of the hexamolybdate (black) compared to compounds **1** (red) and **2** (blue) measured in CH₃CN and (n-Bu₄N)ClO₄ as the supporting electrolyte at scan rate of 100 mV/s. All measurement were referred to Fc/Fc⁺ potential.

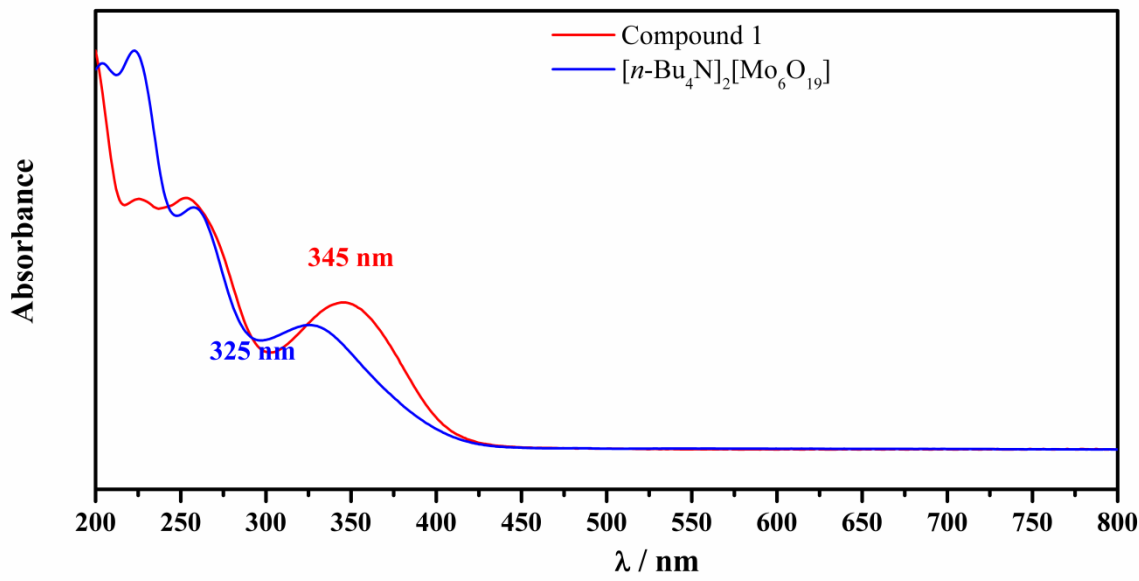


Figure S9. UV-vis absorption spectra of compound **1** (red) and hexamolybdates (blue).

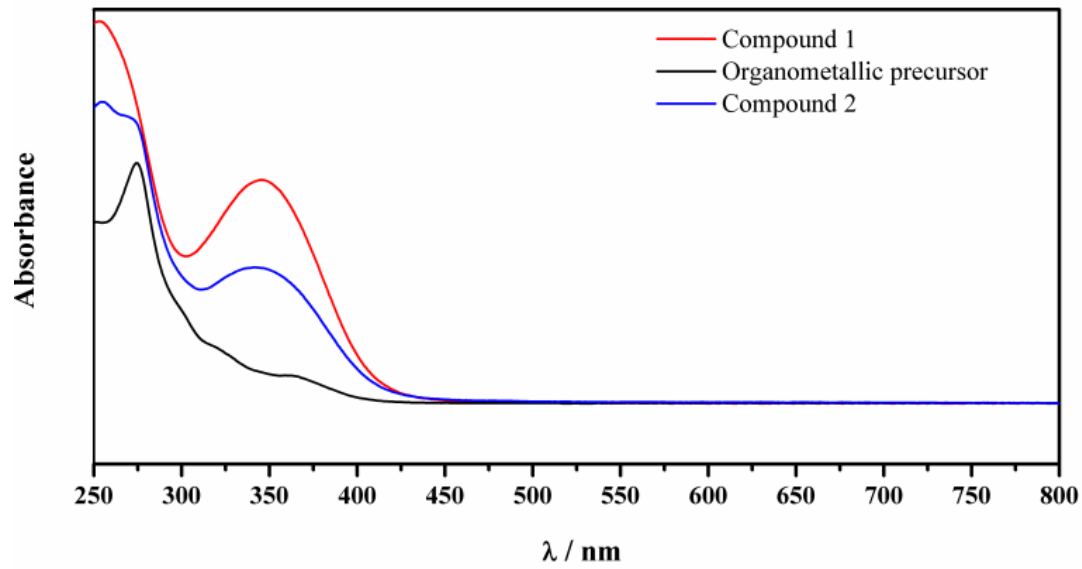


Figure S10. UV-Vis absorption spectra of compound **1** (red), compound **2** (blue) and organometallic precursor (black).

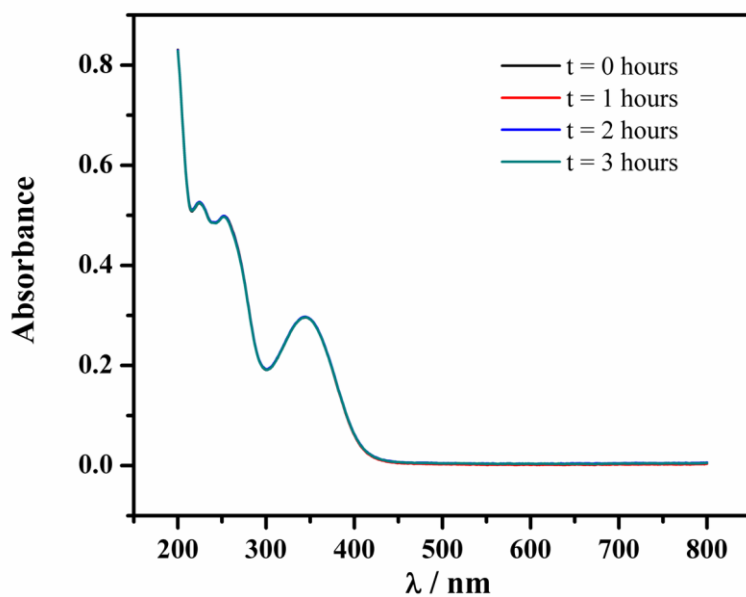


Figure S11. UV-vis absorption spectra of compound **1** exposed to UV irradiation (365 nm) at different times.

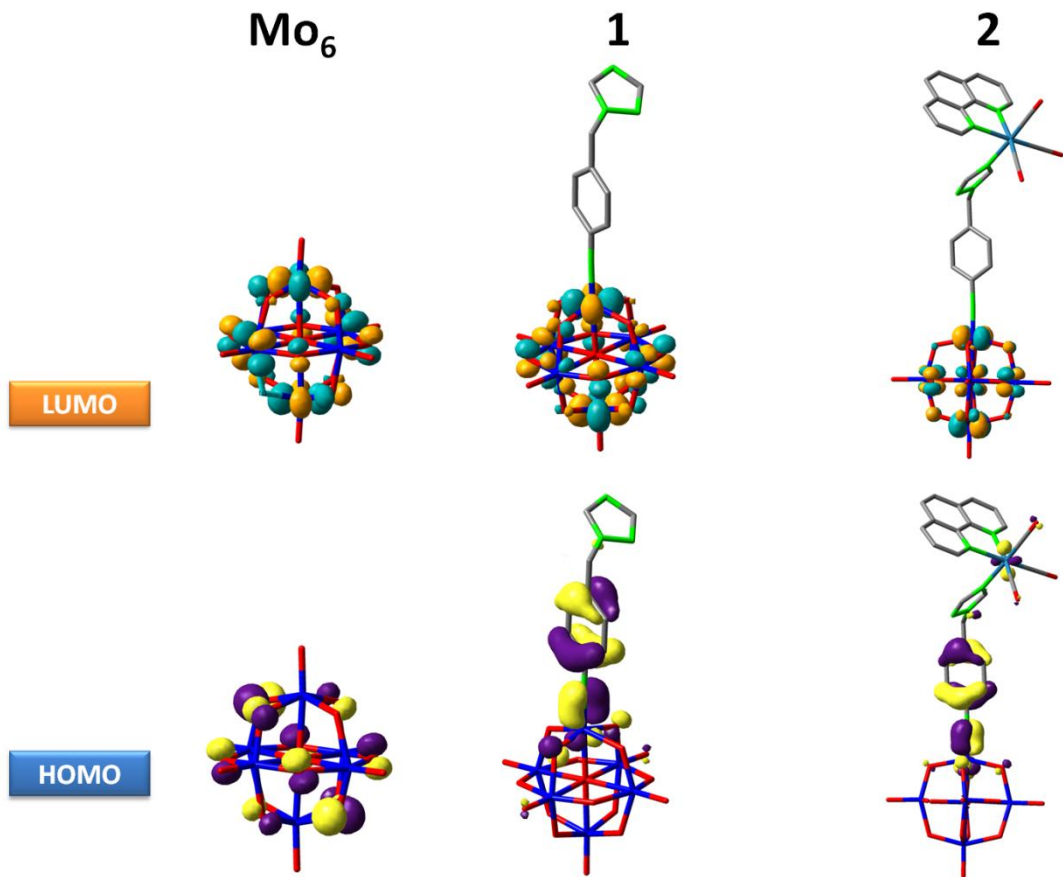


Figure S12. Frontier orbitals surfaces of Mo₆, compounds **1** and **2**.

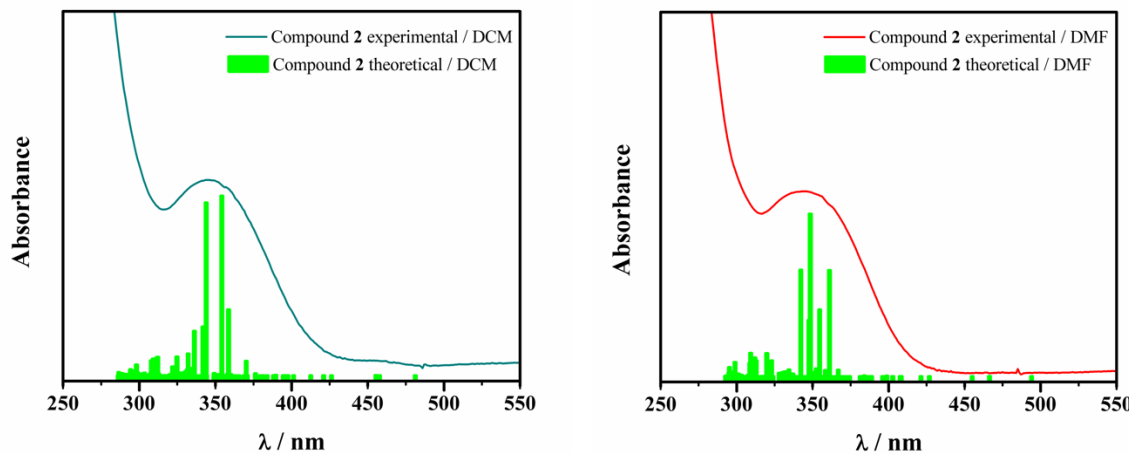


Figure S13. Overlapped plot of experimental spectra and oscillator strength calculated by TD-DFT methods, employing dichloromethane (DCM) and dimethylformamide (DMF) as continuum solvents for compound **2**.